Stars and their variability observed from space
C. Neiner, W. W. Weiss, D. Baade, R. E. Griffin, C. C. Lovekin, A. F. J. Moffat (eds)

BRITE PHOTOMETRIC VARIABILITY OF THE INTRIGUING WOLF-RAYET STAR WR6: ROTATIONAL OR BINARY MODULATIONS?

N. St-Louis[1], A.F.J Moffat[1], T. Ramiaramanantsoa[2] and G. Lenoir-Craig[1]

Abstract. This paper presented preliminary results from a simultaneous photometric and spectroscopic observing campaign of the WR star WR6, of spectral subtype WN4b. The combination of BRITE-Constellation photometry over a time-interval of nearly 160 days and optical spectroscopy over more than 100 days led to a unique dataset, both in time coverage and temporal resolution.

Keywords: Stars: Wolf-Rayet, rotation , winds, outflows

1 Introduction

WR6 is a Wolf-Rayet (WR) star of subtype WN4b; it exhibits a mass-loss rate of $\dot{M}=6.3\times10^{-5}$ $M_{\odot}yr^{-1}$ (Hamann et al. 2019) and a terminal velocity of 1900 kms^{-1} (Prinja et al. 1990). It has long been known to present periodic variability in spectroscopy (e.g. St-Louis et al. 1995; Morel et al. 1997), photometry and polarimetry (e.g. Robert et al. 1992) with a period of 3.77 days but without any clear evidence of a massive companion. Although periodic, the changes have been shown to be *epoch-dependent* (e.g. Robert et al. 1992) and there is therefore certainly a transient phenomenon involved in the process of generating the variability.

The two most common interpretations for the periodic nature of the variability are (a) the presence of large-scale structures in the wind (e.g. St-Louis et al. 2018) in the form of Corotation Interaction Regions (CIRs, Cranmer & Owocki 1995) and (b) a binary system with a low-mass companion (e.g. Schmutz & Koenigsberger 2019). We discuss briefly the BRITE-Constellation observations of WR6 and simultaneous optical spectroscopy obtained by amateur astronomers as members of the Southern Astro Spectroscopy Email Ring (SASER) collaboration.

2 BRITE Photometry

Figure 1 presents the complete light-curve of WR6 obtained between 2015 October 18 and 2016 April 16 by the BRITE-Toronto satellite equipped with a red optical filter. The mean error for these observations is 0.0037 mag. Large-amplitude variability can clearly be seen, with a peak-to-peak amplitude of $\Delta m \sim$0.08.

A period search using the Discrete Fourier Transform technique included in the Period04 package (Lenz & Breger 2005) yielded one independant frequency (ν_1= 0.26712±00013) and at least three different harmonics (ν_2= 0.53199±0.00012, ν_3= 0.78729±0.00016, ν_4= 1.06399±0.00022), indicating (as Fig. 1 shows) that the curve is highly non-sinusoidal. By combining all those harmonics, we calculated a mean period of 3.768 days; we adopt that in this paper.

As the variations are known to be epoch dependent, we carried out a time-frequency analysis of our data using a tapered sliding window covering a time interval of 25 days with an overlap of 50%. We found that the result of this analysis was not very sensitive to either the size of the sliding widow or the overlap interval. Our results are shown in the left panel of Figure 2. The epoch-dependent nature of the variability can clearly be seen, with different combinations of harmonics dominating at different times. The typical stability of a given variability pattern seems to be roughly 30–40 days. The right panel shows a dynamic plot illustrating the evolution of the light-curve as a function of cycle number. Each row presents the light-curve for a given cycle; the magnitudes that are smaller than the global mean are plotted in progressive shades of blue and those higher in progressive shades of red. The curve changes from having one or two peaks whose widths and separation also evolve.

[1] Département de physique, Université de Montréal, C.P. 6128, Succ. Centre-Vile, Montréal (QC), H3C 3J7, Canada
[2] Arizona State University, School of Earth and Space Exploration, 781 Terrace Mall, Rm 770A Tempe, AZ 85287, USA

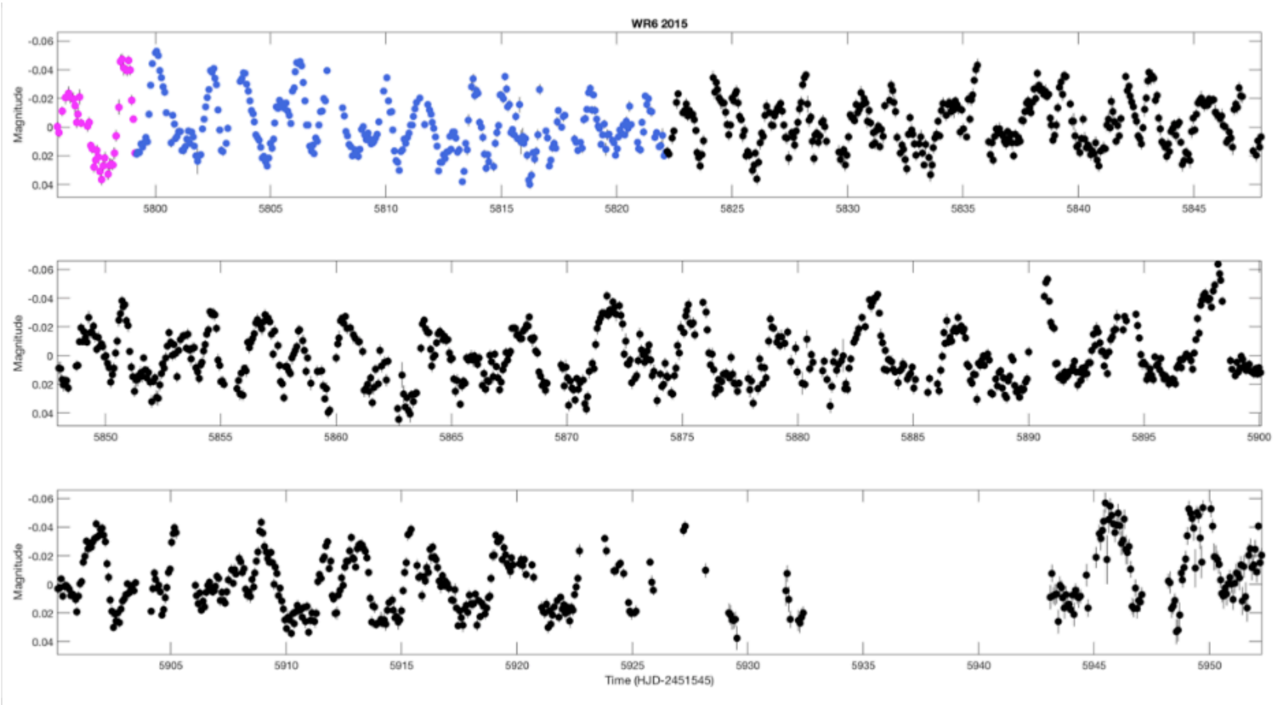

Fig. 1. BRITE light-curve of WR6 obtained by BRITE-Toronto. Satellite-orbital mean fluxes were calculated and the overall mean flux was removed. Various instrument settings (change in the observing conditions; see Popowicz et al. 2017) are plotted in different colours.

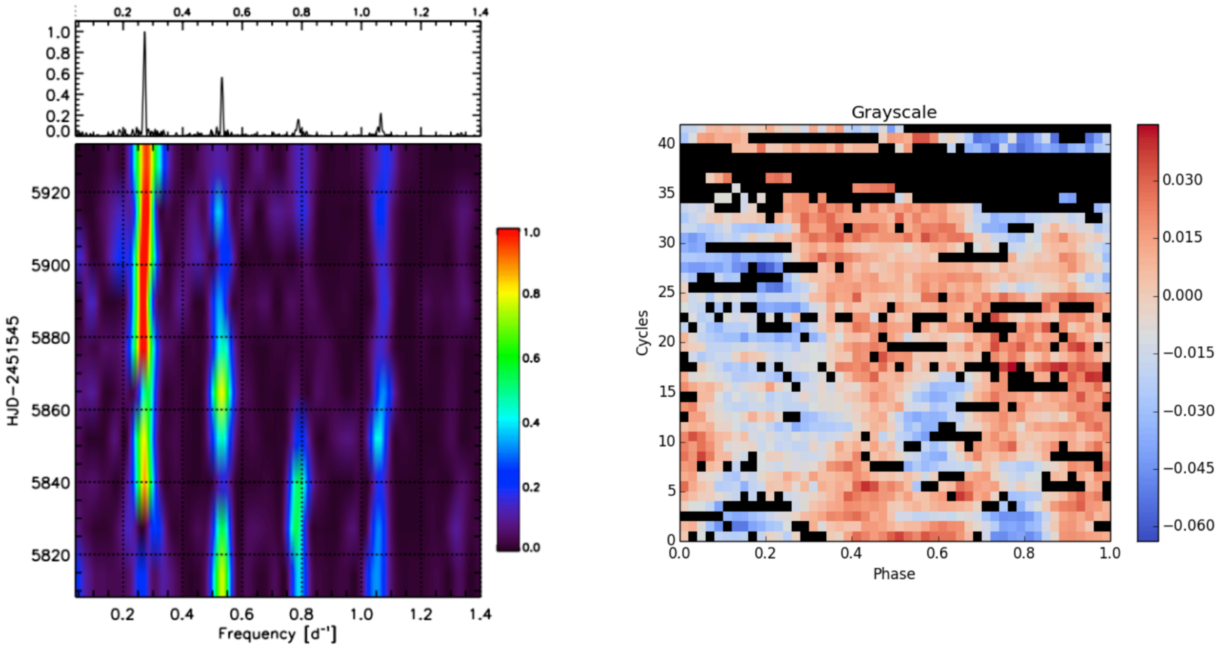

Fig. 2. Left: Time-frequency Fourier transform analysis of our BRITE light-curve of WR6. **Right**: Dynamic plot showing the evolution over time of the periodic variability of WR6. The black regions indicate data gaps.

3 Optical Spectroscopy

Through a fruitful collaboration with a group of four amateur astronomers from the SASER collaboration (Paul Luckas, Paulo Cacella, Bernard Heathcote and Terry C. Bohlsen), we were able to secure 105 optical spectra

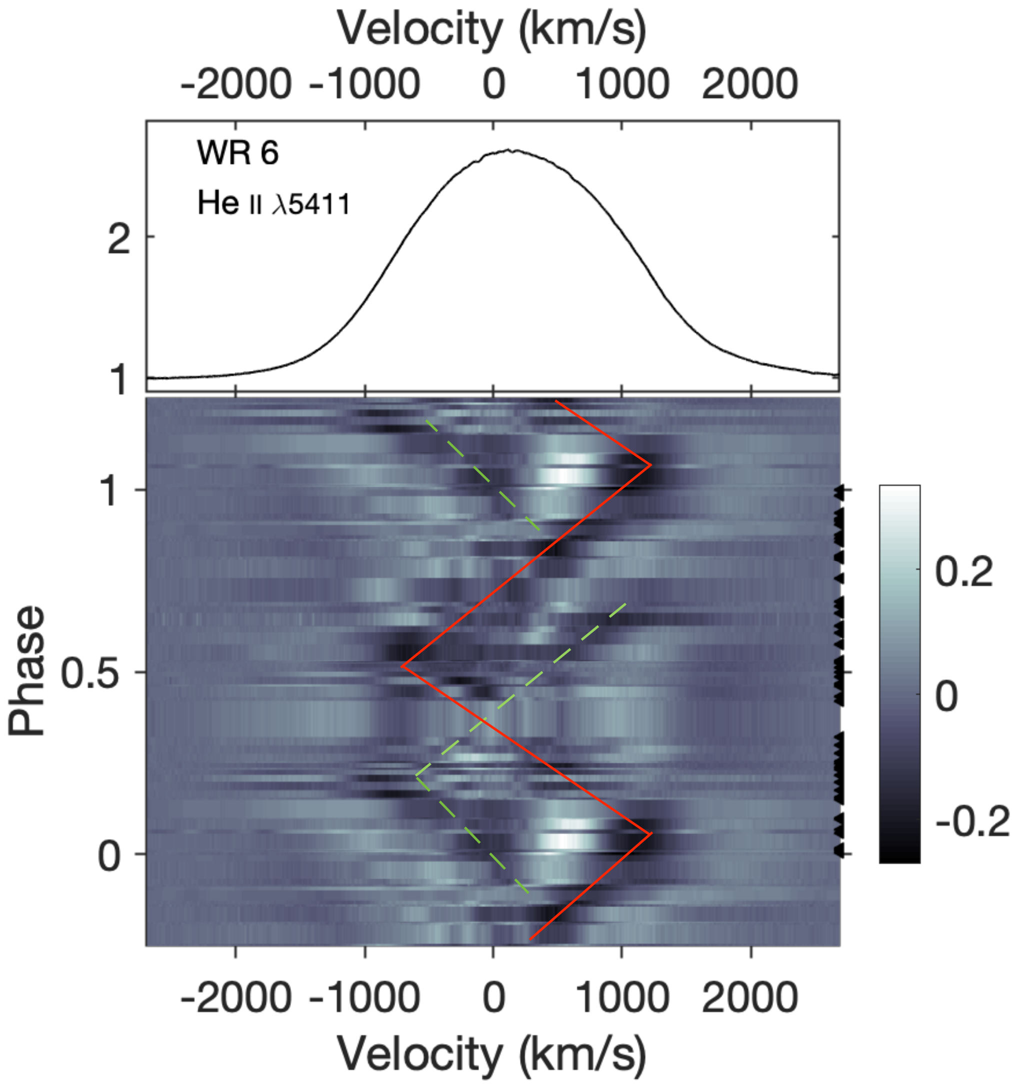

Fig. 3. Dynamic plot showing differences from the global mean of a subset of our optical spectra around the HeIIλ5411 transition as a function of phase of the 3.768-day period.

centred on the HeIIλ5411 emission line between 2016 January 15 to April 28, in parallel with the BRITE observations. A wavelength-dependent CLEAN Fourier analysis of the spectroscopic time-series revealed a period of 3.73$\pm$0.06 days and its first three harmonics across the extent of the HeIIλ5411 line profile, which is compatible – within the errors – with our adopted photometric period. A careful analysis of the spectroscopic variability revealed that the nature of the variability changeed over the 104 days of our observing period. We therefore chose a smaller time-interval to present the spectroscopic variability as a function of phase for our adopted 3.768-day period.

We selected a time-interval of slightly more than 50 days ($\sim$15 cycles of the 3.768-day period) corresponding approximately to the middle panel of Fig. 1. A dynamic plot of the differences between the observed emission lines and the global mean as a function of phase (arbitrary zero point) is presented in Figure 3. The variations are characteristic of the changes expected from CIRs in the wind of a massive star as predicted by Dessart & Chesneau (2002), namely, a characteristic S-Shape feature in the dynamic plot. In our dataset, we found one main dark S-shape feature that reached its maximum negative velocity around phase 0.5 and its maximum positive velocity around phase 0. We have added a red solid line to the plot to indicate the location of that feature. A fainter structure, shifted to lower phases by about 0.2, can also be distinguished (indicated by the dashed green line). During the 15 cycles, most of the light-curve presented only one peak, with a second peak appearing towards the end of the time period (right panel of Figure 2). This is compatible with the variations detected by spectroscopy.

4 Discussion and Conclusions

As mentioned above, the simultaneous photometric and spectroscopic variability we detected during these observations had characteristics that are compatible with CIRs in the wind of a massive star. The periodic but epoch-dependent nature of the variability, the presence of a number of harmonics associated with the periodic phenomenon, and the spectroscopic characteristics of the line-profile changes, are all expected within the framework of that model.

The binary scenario presented by Schmutz & Koenigsberger (2019) involves light variations with an orbital period of 3.63 days and a fast apsidal motion from a putative third star on a timescale of ∼100 days. The resulting sidereal period is the well-known 3.77-day period. The variability is mostly caused by two eclipses per cycle by either the WR star (20 $M_\odot$) or its yet undetected low-mass companion (1.5 $M_\odot$), of shocked WR wind as it collides with the surface of its low mass companion, contributing about 15% of the total flux. To estimate the minimum period of the outer body causing the fast apsidal motion, one must assume a mass for this third body. If the mass of the third body is equal to that of the WR star, the outer period is estimated to $P_{\rm out}$=22 days, while if the mass of the third body dominates, the outer period would be 31 days. We note that there is no sign of such periods from a period-search analysis.

A more careful analysis is required to determine which model reproduces best the entirety of the data obtained for this star over the years. The correlated ultraviolet continuum and line-flux variability accompanied by blue edge P Cygni absorption component changes (St-Louis et al. 1995), the broadband continuum polarimetric variability (e.g. St-Louis et al. 2018), the correlated optical continuum and line flux changes (e.g. Morel et al. 1997) and the lack of correlation between the optical photometric changes and X-ray variability (Huenemoerder et al. 2015) are examples of phenomena that will need to be reproduced by the models.

References

Cranmer, S. R. & Owocki, S. P. 1995, ApJ, 440, 308

Dessart, L. & Chesneau, O. 2002, A&A, 395, 209

Hamann, W. R., Gräfener, G., Liermann, A., et al. 2019, A&A, 625, A57

Huenemoerder, D. P., Gayley, K. G., Hamann, W.-R., et al. 2015, ApJ, 815, 29

Lenz, P. & Breger, M. 2005, Communications in Asteroseismology, 146, 53

Morel, T., St-Louis, N., & Marchenko, S. V. 1997, ApJ, 482, 470

Popowicz, A., Pigulski, A., Bernacki, K., et al. 2017, A&A, 605, A26

Prinja, R. K., Barlow, M. J., & Howarth, I. D. 1990, ApJ, 361, 607

Robert, C., Moffat, A. F. J., Drissen, L., et al. 1992, ApJ, 397, 277

Schmutz, W. & Koenigsberger, G. 2019, A&A, 624, L3

St-Louis, N., Dalton, M. J., Marchenko, S. V., Moffat, A. F. J., & Willis, A. J. 1995, ApJ, 452, L57

St-Louis, N., Tremblay, P., & Ignace, R. 2018, MNRAS, 474, 1886